

Brönsted acid on Beta zeolite induced the high-efficiency of the amidation of styrene in the aqueous phase

Jiteng Liu, Xueqin Jia, Lei Zhang, Wenqian Fu*

Jiangsu Key Laboratory of Advanced Catalytic Materials and Technology, School of
Petrochemical Engineering, Changzhou University, Changzhou, Jiangsu 213164, P. R.
China.

* Corresponding author.

E-mail address: fuwenqian@cczu.edu.cn (W. Fu)

1. Sialylation of H-Mbeta

To investigate the effect of hydrophilicity and hydrophobicity of the material on this reaction,^{1,2} the H-MBeta was treated with sialylation using a trimethylchlorosilane as a reagent. As a typical run, 0.2 g trimethylchlorosilane was dissolved in 20 mL ethanol, followed by 1 g H-MBeta was added into above solution and stirred at 80 °C for 4 h. After completion of silylanization. The mixture was centrifuged, washed with ethanol, dried at 100 °C overnight and calcined at 450 °C for 4 h. The resulting sample was denoted as Hy-H-MBeta.

To diagnose the hydrophobicity of dired Hy-H-MBeta, this sample and parent H-MBeta were characterized by diffuse reflection infrared spectroscopy. Before measurement, the samples were pretreated for 2 hours in an *in situ* cell under a vacuum at 200 °C and then cooled to 50 °C. The infrared spectra were collected using KBr as background.

2 Recycle performance of the catalyst

To evaluate the recycle performance of the catalyst, considering that the catalyst would be inevitably lost during the recovery process, a series of parallel experiments of the H-MBeta sample were performed. Firstly, sever 10 mL sealed Schlenk tubes, each charged into catalyst and reactants (40 mg catalyst, 0.2 mmol styrene, 0.7 mmol benzonitrile, 1 mL of H₂O), were placed in reaction tray at 100 °C for 12 h. When the reaction was finished, these catalysts were meticulously isolated from the reaction mixture through centrifugation, and then thoroughly mixed and washed with water. After that, the collected sample was dried at 100 °C for 12 h and calcined at 550 °C for 4 h in an air atmosphere before being used in the next cycle. Because the inevitable loss of the catalyst occurred during catalyst washing and transfer, the amount of the collected catalyst was reduced. The remaining catalysts were evaluated in the parallel experiments. After 5 runs for the catalyst, the catalyst was denoted as S-H-MBeta, which was characterized by XRD patterns, N₂ adsorption-desorption isotherm, NH₃-TPD curves and Py-IR spectra.

2. Figures

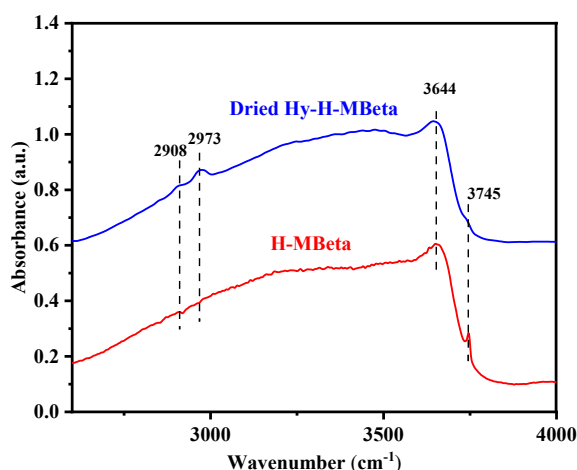


Fig. S1. The diffuse reflection infrared spectra of H-MBeta and dried Hy-H-MBeta samples.

Discussion:

In order to diagnose the hydrophobicity of dried Hy-H-MBeta, this sample and parent H-MBeta were characterized by infrared spectroscopy. As shown in Fig. S1, the infrared spectrum of the parent H-MBeta can distinguish two infrared absorption bands in the region of 2600 - 4000 cm⁻¹. The absorption band at 3745 cm⁻¹ was assigned to the end-terminal silanol, and the absorption peak at 3644 cm⁻¹ corresponded to the acidic bridged hydroxyl group (Al(OH)Si) bonding to the framework.^{1, 3} Hy-H-MBeta had three infrared absorption bands in this region. The intensity of band at 3745 cm⁻¹ was significantly reduced, and new bands at 2908 and 2973 cm⁻¹ associated with C-H bond stretching vibration from trimethylchlorosilane appeared, which proves that the reaction of trimethylchlorosilane with terminal silanol greatly reduces the silanols. While the band at 3644 cm⁻¹ was slightly reduced, which indicated that the hydrolyzed trimethylchlorosilane was prior to react with the silanols.

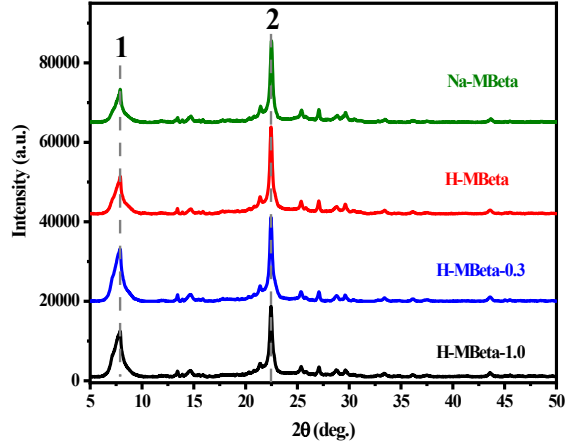


Fig. S2. XRD patterns of the series of mesoporous Beta zeolite samples.

Discussion:

The relative crystallinities of the samples were calculated by comparing the sums of the peak height at $2\theta=7.9$ and 22.4° the sample to that of Na-MBeta sample. Specifically,

$$Crystallinity (\%) = \frac{\sum_{i=1}^2 I_{i.sample}}{\sum_{i=1}^2 I_{i.reference}} \times 100\% \quad (1)$$

In Equation 1, $I_{i, sample}$ represents the peak height $2\theta=7.9$ and 22.4° for the series mesoporous Beta zeolite and $I_{i, reference}$ represents the peak height $2\theta=7.9$ and 22.4° for the reference Na-MBeta zeolite. Figure 10 showed the XRD patterns of the series mesoporous Beta zeolite samples. The diffraction peak at $2\theta=7.9$ and 22.4° was marked with dotted line. The specific calculation process is as follows:

$$H-MBeta: C \quad rystallinity (\%) = \frac{9775.76 + 12718.1}{8147.28 + 10140.41} \times 100\% = 123\%$$

$$H-MBeta-0.3: C \quad rystallinity (\%) = \frac{14622.32 + 11567.13}{8147.28 + 10140.41} \times 100\% = 143\%$$

$$H-MBeta-1.0: C \quad rystallinity (\%) = \frac{12716.34 + 9819.13}{8147.28 + 10140.41} \times 100\% = 123\%$$

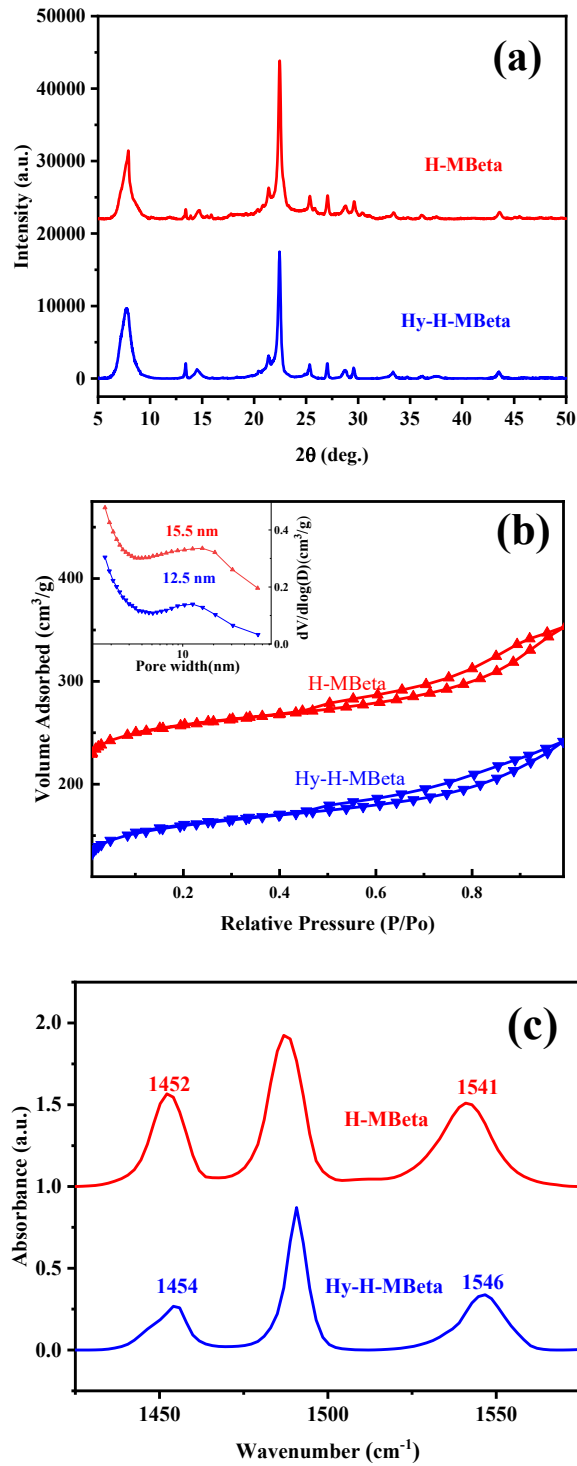


Fig. S3. (a) XRD patterns, (b) N₂ adsorption-desorption isotherm and (c) Py-IR spectra of H-MBeta and Hy-H-MBeta.

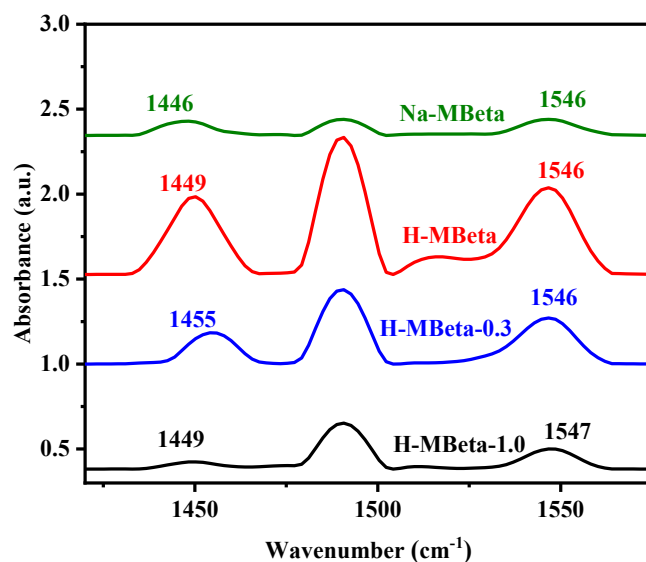


Fig. S4. (a) Py-IR spectra of sample adsorbed pyridine (The self-supporting wafer (approximate 20 mg) of the sample was pretreated in an *in-situ* cell at 400 °C for 2 h under a vacuum and then was cooled to 50 °C. Pyridine vapor was introduced into *in situ* cell in N₂ stream until adsorption saturation at 50 °C. The spectrum was recorded at 50 °C in deduction of the sample backing spectrum after desorption of pyridine at 350 °C under vacuum of 10⁻² Pa.)

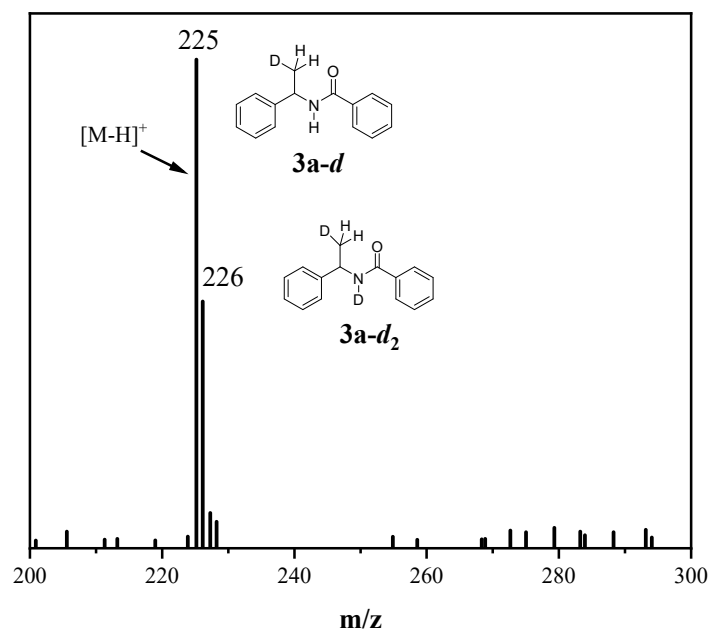


Fig. S5. LCMS spectra of **3a-d** and **3a-d₂** (The Ritter reaction of styrene with benzonitrile was performed in deuterium water, a mixture of products **3a-d** and **3a-d₂** were obtained, which was analyzed by LCMS, as shown in Fig.S5).

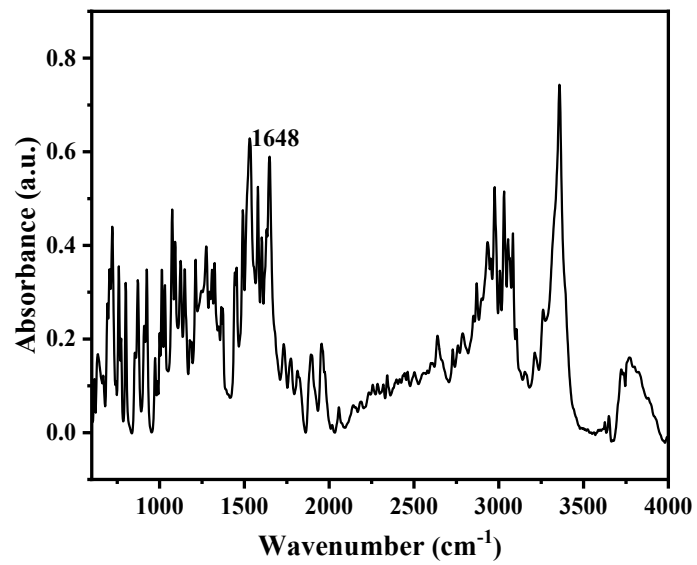


Fig. S6. Diffuse reflection infrared spectrum of the *N*-(1-phenylethyl) benzamide product.

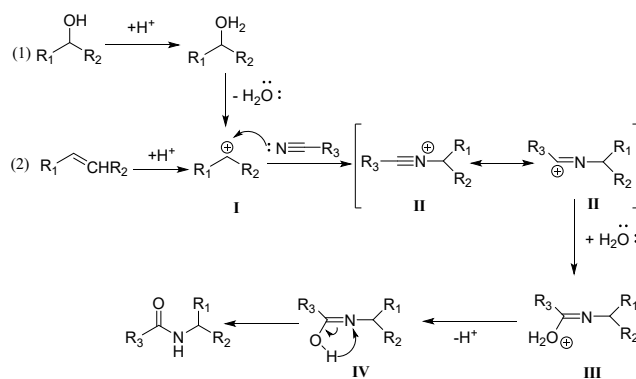


Fig. S7. The general mechanism proposed by research workers in the published works.³⁻

8

Discussion:

Many researchers developed various Brönsted or Lewis acid catalysts, and proposed widely accepted and unanimous reaction mechanism, as shown in Fig. S7. Alcohol was protonated by the protonic acid, releasing a water molecule to form a carbocation (**I**). While the alkene was directly protonated to form a carbocation (**I**). The lone electron pair of the nitrile group attacks this cation to form nitrilium ion (**II**). Another lone electron pair of the oxygen atom in the water molecule attacks the nitrilium ion to form intermediate **III** that was subsequently underwent proton elimination process and transformed into intermediate **IV**. This intermediate **IV** tautomerizes to generate more stable *N*-alkylated amides.

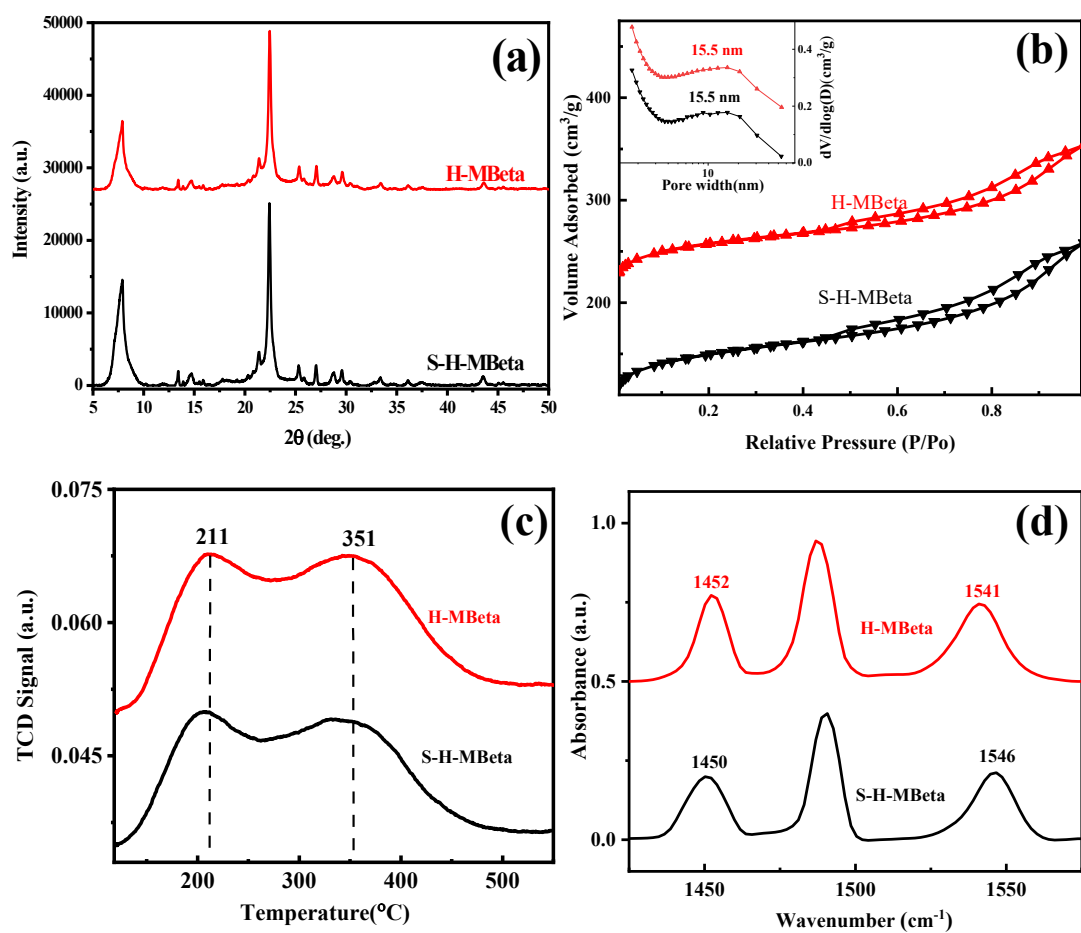


Fig. S8 (a) XRD patterns, (b) N_2 adsorption-desorption isotherms, (c) NH_3 -TPD curves and (d) Py-IR spectra of H-MBeta and S-H-MBeta.

3. Tables

Table S1. Screening of different temperature for the amination of styrene with benzonitrile. ^a

Entry	Temperature	Conversion (%) ^b	Product selectivity. (%) ^c
1	70	30	78
2	80	43	85
3	100	87	90
4	120	83	89
5	150	87	69

^a Reaction conditions: 0.2 mmol **1a**, 0.7 mmol **2a**, 1 mL H₂O, air, 40 mg zeolite catalyst, 12 h. ^{b,c} the conversion of styrene and product selectivity were analyzed by GC.

Table S2. Screening of different time for the amination of styrene with benzonitrile. ^a

Entry	Time	Conversion (%) ^b	Product selectivity (%) ^c
1	8	61	87
2	10	73	89
3	12	87	90
4	14	82	86
5	16	85	88
6	18	86	90

^a Reaction conditions: 0.2 mmol **1a**, 0.7 mmol **2a**, 1 mL H₂O, air, 40 mg zeolite catalyst and 100 °C. ^{b,c} the conversion of styrene and product selectivity were analyzed by GC.

Table S3. Screening of different solvent for the amination of styrene with benzonitrile.
a

Entry	Solvent	Conversion (%) ^b	Product selectivity (%) ^c
1	THF	-	-
2	DCE	-	-
3	cyclohexane	-	-
4	1, 4-dioxane	-	-
5	DMSO	-	-
6	DMF	-	-
7	toluene	-	-
8	ethanol	-	-
9	H ₂ O	87	90

^a Reaction conditions: 0.2 mmol **1a**, 0.7 mmol **2a**, 1 mL solvent, air, 40 mg zeolite catalyst, 12 h and 100 °C. ^{b,c} the conversion of styrene and product selectivity were analyzed by GC.

Table S4. Screening of different amounts of water for the amination of styrene with benzonitrile. ^a

Entry	Amounts of water (mL)	Conversion (%) ^b	Product selectivity (%) ^c
1	0.5	63	61
2	0.8	65	93
3	1.0	89	90
4	1.2	84	81

^a Reaction conditions: 0.2 mmol **1a**, 0.7 mmol **2a**, H₂O, air, 40 mg zeolite catalyst, 12 h and 100 °C. ^{b,c} the conversion of styrene and product selectivity were analyzed by GC.

Table S5. Screening of the molar ratio of styrene to benzonitrile in the Ritter reaction.^a

Entry	Styrene: Benzonitrile	Conversion (%) ^b	Product selectivity (%) ^c
1	1:1	71	55
2	1:1.5	80	57
3	1:2	86	73
4	1:2.5	85	78
5	1:3	83	85
6	1:3.5	87	90
7	1:4	86	88
8	1:4.5	87	88
9	1:5	72	85

^a Reaction conditions: 0.2 mmol **1a**, 1 mL H₂O, air, 40 mg zeolite catalyst, 12 h and 100 °C. ^{b,c} the conversion of styrene and product selectivity were analyzed by GC.

Table S6. Screening of different atmosphere for the amination of styrene with benzonitrile. ^a

Entry	Atmosphere	Conversion (%) ^b	Product selectivity (%) ^c
1	Air	87	90
2	N ₂	81	91
3	O ₂	85	89

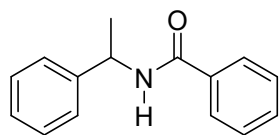
^a Reaction conditions: 0.2 mmol **1a**, 0.7 mmol **2a**, 1 mL H₂O, 40 mg zeolite catalyst, 12 h and 100 °C. ^{b,c} the conversion of styrene and product selectivity were analyzed by GC.

Table S7. Strong acid content and acid site distribution of catalyst. ^a

Samples	Amount (μmol·g ⁻¹) and distribution of acid sites			
	B ^b	L ^b	B+L	B/L
Na-MBeta	54	30	84	1.8
H-MBeta	156	89	245	1.8
H-MBeta-0.3	106	66	172	1.6
H-MBeta-1.0	73	25	98	2.9

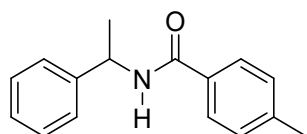
^a Strong acid content and acid site distribution of catalyst treated at 350 °C.

3. Characterization of the products



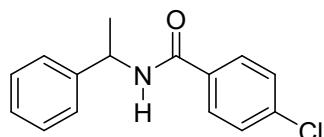
N-(1-phenylethyl)benzamide: white solid

¹H NMR (400 MHz, CDCl₃) δ 7.68 (dd, *J* = 7.0, 1.6 Hz, 2H), 7.39 (t, *J* = 7.4 Hz, 1H), 7.34 – 7.24 (m, 6H), 7.21 – 7.16 (m, 1H), 6.41 (d, *J* = 7.7 Hz, 1H), 5.25 (p, *J* = 7.1 Hz, 1H), 1.51 (d, *J* = 6.9 Hz, 3H).



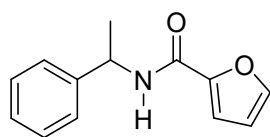
4-methyl-N-(1-phenylethyl)benzamide: white solid

¹H NMR (400 MHz, CDCl₃) δ 7.58 (d, *J* = 8.2 Hz, 2H), 7.31 – 7.22 (m, 4H), 7.19 – 7.15 (m, 1H), 7.10 (d, *J* = 7.9 Hz, 2H), 6.41 (d, *J* = 7.9 Hz, 1H), 5.23 (p, *J* = 7.1 Hz, 1H), 2.28 (s, 3H), 1.49 (d, *J* = 6.9 Hz, 3H).



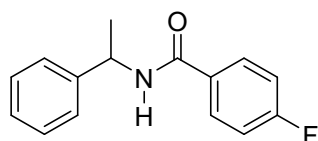
4-chloro-N-(1-phenylethyl)benzamide: white solid

¹H NMR (400 MHz, CDCl₃) δ 7.62 (d, *J* = 8.2 Hz, 2H), 7.29 (dd, *J* = 6.0, 2.9 Hz, 6H), 7.26 – 7.19 (m, 1H), 6.34 (d, *J* = 7.7 Hz, 1H), 5.23 (p, *J* = 7.1 Hz, 1H), 1.52 (d, *J* = 6.9 Hz, 3H).



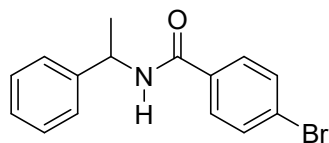
N-(1-phenylethyl)furan-2-carboxamide: white solid

¹H NMR (400 MHz, DMSO) δ 8.74 (d, *J* = 8.3 Hz, 1H), 7.84 (dd, *J* = 1.8, 0.8 Hz, 1H), 7.38 (d, *J* = 5.2 Hz, 2H), 7.32 (t, *J* = 7.6 Hz, 2H), 7.22 (t, *J* = 7.2 Hz, 1H), 7.15 (d, *J* = 2.6 Hz, 1H), 6.62 (dd, *J* = 3.4, 1.8 Hz, 1H), 5.13 (dt, *J* = 14.1, 7.2 Hz, 1H), 1.47 (d, *J* = 7.1 Hz, 3H).



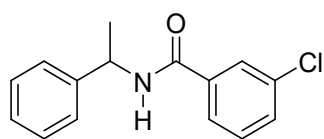
4-fluoro-N-(1-phenylethyl)benzamide: white solid

$^1\text{H NMR}$ (400 MHz, CDCl_3) δ 7.69 (dd, $J = 8.6, 5.3$ Hz, 2H), 7.31 – 7.15 (m, 5H), 6.99 (t, $J = 8.5$ Hz, 2H), 6.36 (d, $J = 7.7$ Hz, 1H), 5.23 (p, $J = 7.1$ Hz, 1H), 1.51 (d, $J = 6.9$ Hz, 3H).



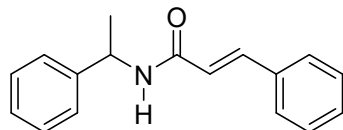
4-bromo-N-(1-phenylethyl)benzamide: white solid

$^1\text{H NMR}$ (400 MHz, CDCl_3) δ 7.55 (d, $J = 8.6$ Hz, 2H), 7.45 (d, $J = 8.5$ Hz, 2H), 7.34 – 7.15 (m, 5H), 6.34 (d, $J = 7.8$ Hz, 1H), 5.22 (p, $J = 7.1$ Hz, 1H), 1.52 (d, $J = 7.0$ Hz, 3H).



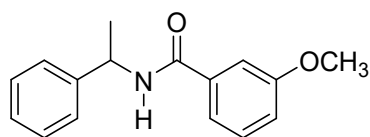
3-chloro-N-(1-phenylethyl)benzamide: white solid

$^1\text{H NMR}$ (400 MHz, CDCl_3) δ 7.66 (t, $J = 1.9$ Hz, 1H), 7.54 (d, $J = 7.7$ Hz, 1H), 7.36 (ddd, $J = 8.0, 2.1, 1.1$ Hz, 1H), 7.29 – 7.17 (m, 6H), 6.43 (d, $J = 7.6$ Hz, 1H), 5.22 (p, $J = 7.1$ Hz, 1H), 1.51 (d, $J = 6.9$ Hz, 3H).



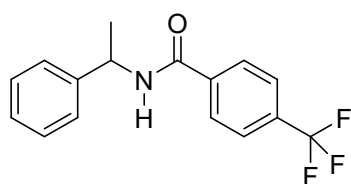
N-(1-phenylethyl)cinnamamide: white solid

$^1\text{H NMR}$ (400 MHz, CDCl_3) δ 7.55 (d, $J = 15.6$ Hz, 1H), 7.37 (dd, $J = 6.6, 2.9$ Hz, 2H), 7.31 – 7.17 (m, 8H), 6.36 (d, $J = 15.6$ Hz, 1H), 6.13 (d, $J = 8.1$ Hz, 1H), 5.19 (p, $J = 7.1$ Hz, 1H), 1.47 (d, $J = 6.9$ Hz, 3H).



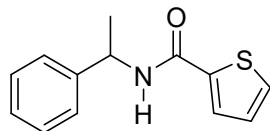
3-methoxy-N-(1-phenylethyl)benzamide: white solid

$^1\text{H NMR}$ (400 MHz, CDCl_3) δ 7.30 – 7.16 (m, 8H), 6.93 (dt, $J = 6.8, 2.6$ Hz, 1H), 6.39 (d, $J = 7.6$ Hz, 1H), 5.24 (p, $J = 7.1$ Hz, 1H), 3.73 (s, 3H), 1.51 (d, $J = 6.9$ Hz, 3H).



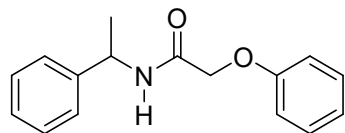
N-(1-phenylethyl)-4-(trifluoromethyl)benzamide: white solid

$^1\text{H NMR}$ (400 MHz, CDCl_3) δ 7.75 (d, $J = 8.0$ Hz, 2H), 7.53 (d, $J = 8.0$ Hz, 2H), 7.29 – 7.16 (m, 5H), 6.62 (d, $J = 7.4$ Hz, 1H), 5.22 (p, $J = 7.1$ Hz, 1H), 1.51 (d, $J = 6.9$ Hz, 3H).



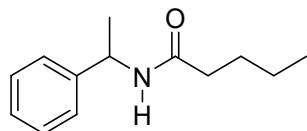
N-(1-phenylethyl)thiophene-2-carboxamide: white solid

$^1\text{H NMR}$ (400 MHz, CDCl_3) δ 7.59 (d, $J = 4.0$ Hz, 1H), 7.41 (d, $J = 7.7$ Hz, 1H), 7.36 (d, $J = 5.1$ Hz, 1H), 7.34 – 7.29 (m, 2H), 7.23 (t, $J = 7.6$ Hz, 2H), 7.15 (t, $J = 7.2$ Hz, 1H), 6.95 (t, $J = 4.4$ Hz, 1H), 5.20 (p, $J = 7.1, 6.7$ Hz, 1H), 1.48 (d, $J = 7.0$ Hz, 3H).



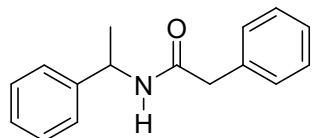
2-phenoxy-N-(1-phenylethyl)acetamide: white solid

$^1\text{H NMR}$ (400 MHz, CDCl_3) δ 7.30 – 7.15 (m, 7H), 6.94 (t, $J = 7.4$ Hz, 1H), 6.83 (dd, $J = 8.8, 1.0$ Hz, 2H), 6.74 (d, $J = 8.1$ Hz, 1H), 5.20 – 5.11 (m, 1H), 4.47 – 4.35 (m, 2H), 1.45 (d, $J = 6.9$ Hz, 3H).



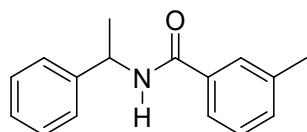
N-(1-phenylethyl)pentanamide: white solid

$^1\text{H NMR}$ (400 MHz, DMSO) δ 8.23 (s, 1H), 7.33 – 7.19 (m, 5H), 4.97 – 4.85 (m, 1H), 2.07 (dt, $J = 30.1, 7.5$ Hz, 2H), 1.47 (p, $J = 7.5$ Hz, 2H), 1.32 (d, $J = 7.1$ Hz, 3H), 1.28 – 1.21 (m, 2H), 0.86 (td, $J = 7.3, 2.7$ Hz, 3H).



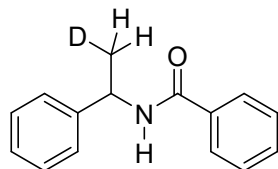
2-phenyl-N-(1-phenylethyl)acetamide: white solid

$^1\text{H NMR}$ (400 MHz, CDCl_3) δ 7.26 – 7.08 (m, 10H), 5.83 (d, $J = 9.1$ Hz, 1H), 5.02 (p, $J = 7.1$ Hz, 1H), 3.46 (s, 2H), 1.30 (d, $J = 7.0$ Hz, 3H).



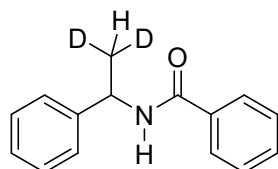
3-methyl-N-(1-phenylethyl)benzamide: white solid

$^1\text{H NMR}$ (400 MHz, CDCl_3) δ 7.50 (s, 1H), 7.46 (d, $J = 4.9$ Hz, 1H), 7.30 – 7.19 (m, 4H), 7.16 (d, $J = 5.2$ Hz, 3H), 6.58 (s, 1H), 5.21 (p, $J = 7.1$ Hz, 1H), 2.24 (s, 3H), 1.47 (d, $J = 6.9$ Hz, 3H).



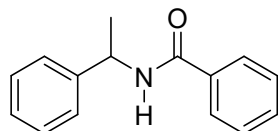
3a-d: white solid

$^1\text{H NMR}$ (400 MHz, CDCl_3) δ 7.70 (d, $J = 7.0$ Hz, 2H), 7.45 – 7.17 (m, 8H), 6.31 (d, $J = 7.7$ Hz, 1H), 5.42 – 5.12 (m, 1H), 1.52 (d, $J = 6.9$ Hz, 2H).



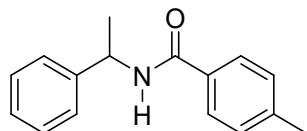
3a-d₂: white solid

$^1\text{H NMR}$ (300 MHz, CDCl_3) δ 7.70 (d, $J = 7.4$ Hz, 2H), 7.57 – 7.05 (m, 8H), 6.29 (s, 1H), 5.25 (d, $J = 7.8$ Hz, 1H), 1.52 (d, $J = 5.4$ Hz, 1H).



N-(1-phenylethyl)benzamide: white solid

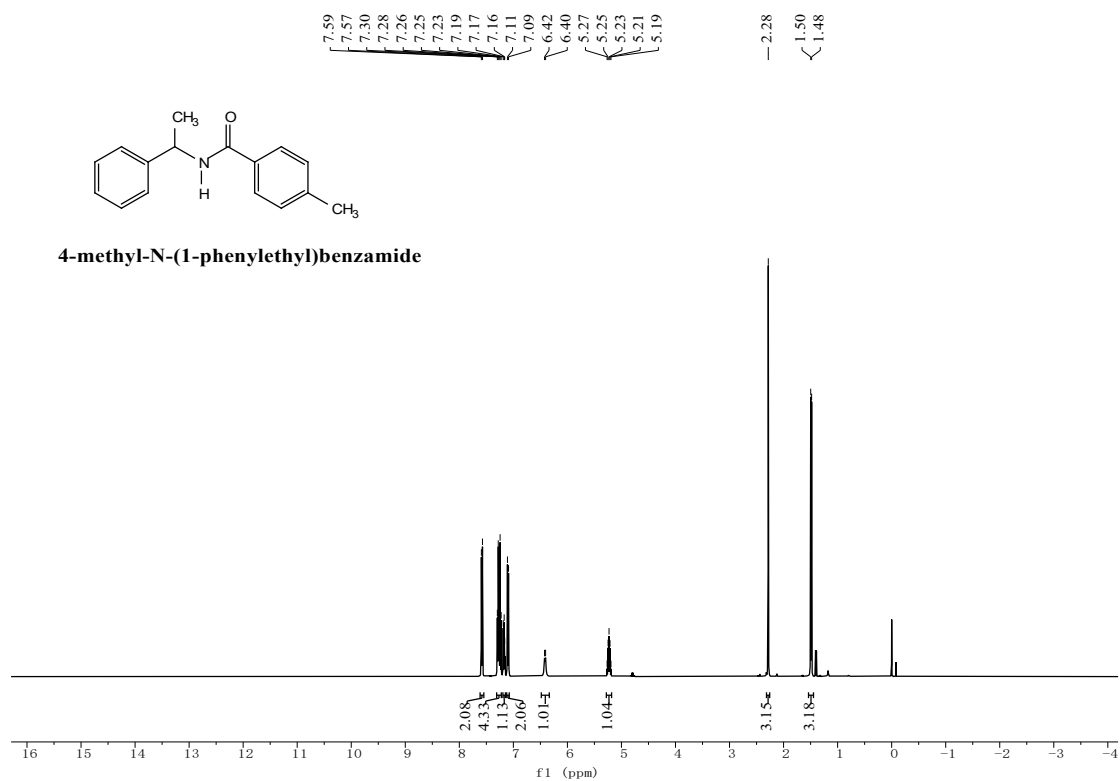
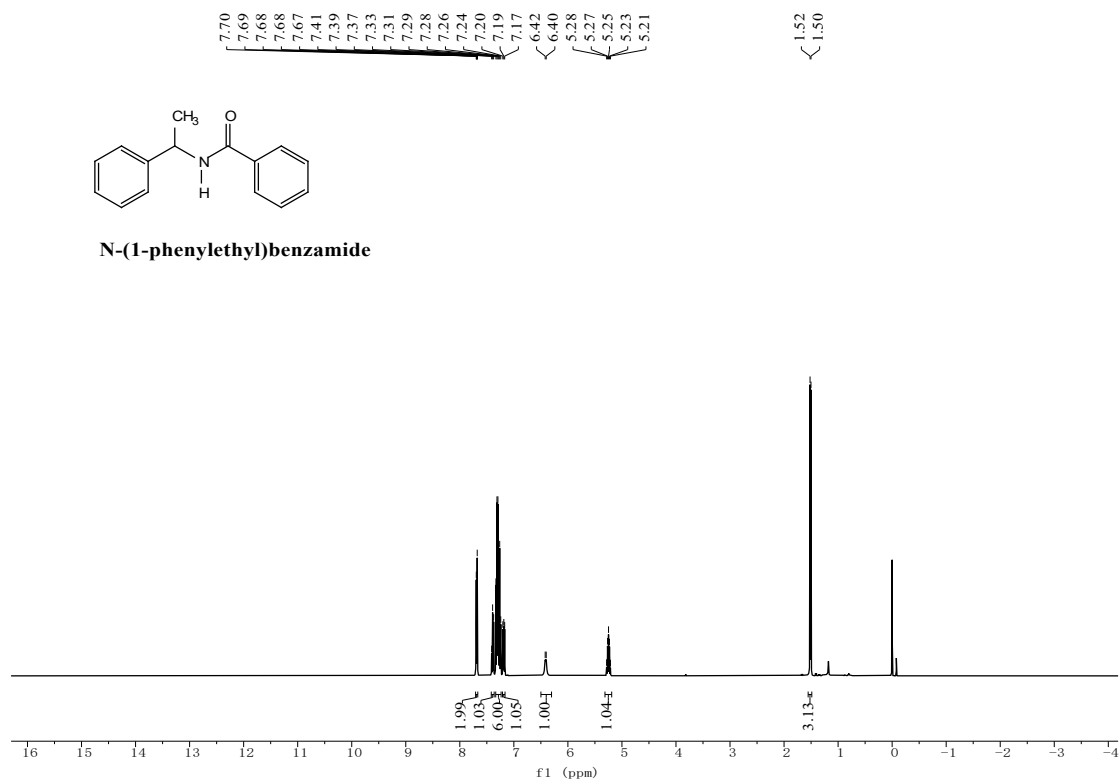
$^1\text{H NMR}$ (300 MHz, CDCl_3) δ 7.69 (d, $J = 6.6$ Hz, 2H), 7.40 (t, $J = 7.2$ Hz, 1H), 7.29 (p, $J = 7.5$ Hz, 6H), 7.18 (d, $J = 4.2$ Hz, 1H), 6.40 (s, 1H), 5.25 (p, $J = 7.1$ Hz, 1H), 1.51 (d, $J = 6.9$ Hz, 3H).

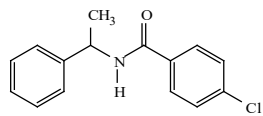


4-methyl-N-(1-phenylethyl)benzamide: white solid

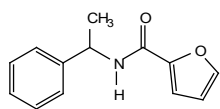
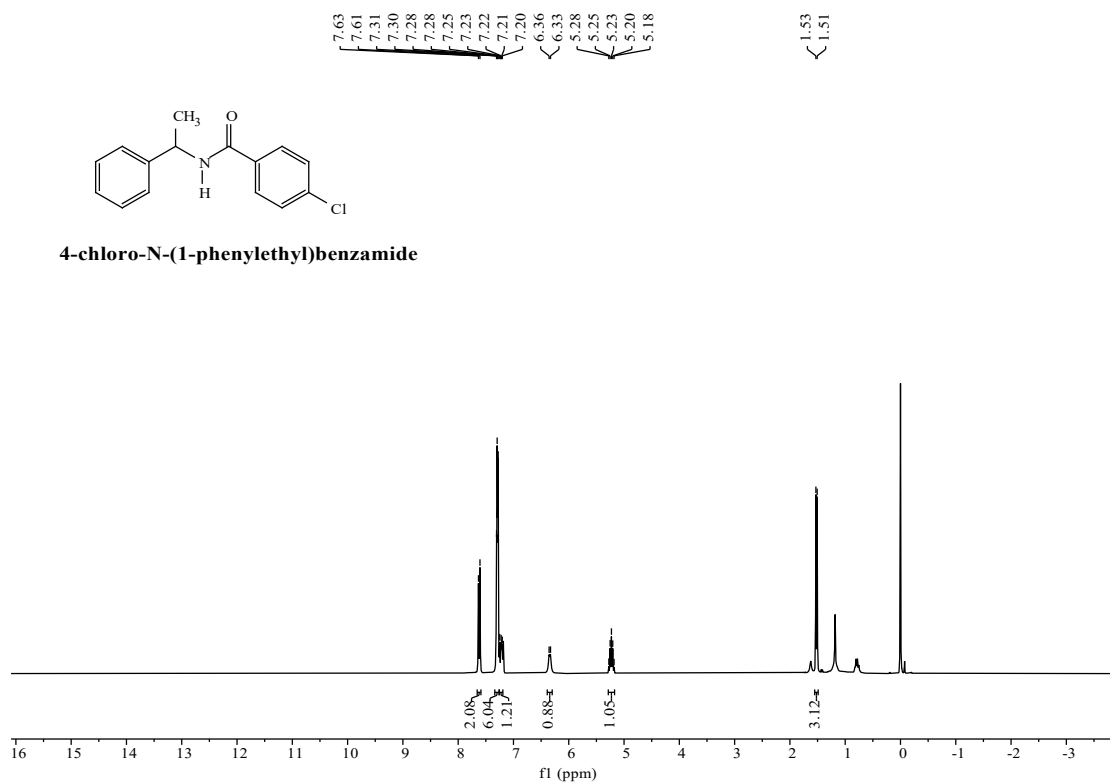
$^1\text{H NMR}$ (300 MHz, CDCl_3) δ 7.59 (d, $J = 7.8$ Hz, 2H), 7.42 – 7.18 (m, 5H), 7.14 (d, $J = 7.9$ Hz, 2H), 6.45 (s, 1H), 5.26 (p, $J = 7.1$ Hz, 1H), 2.31 (s, 3H), 1.52 (d, $J = 6.9$ Hz, 3H).

4. The NMR spectra

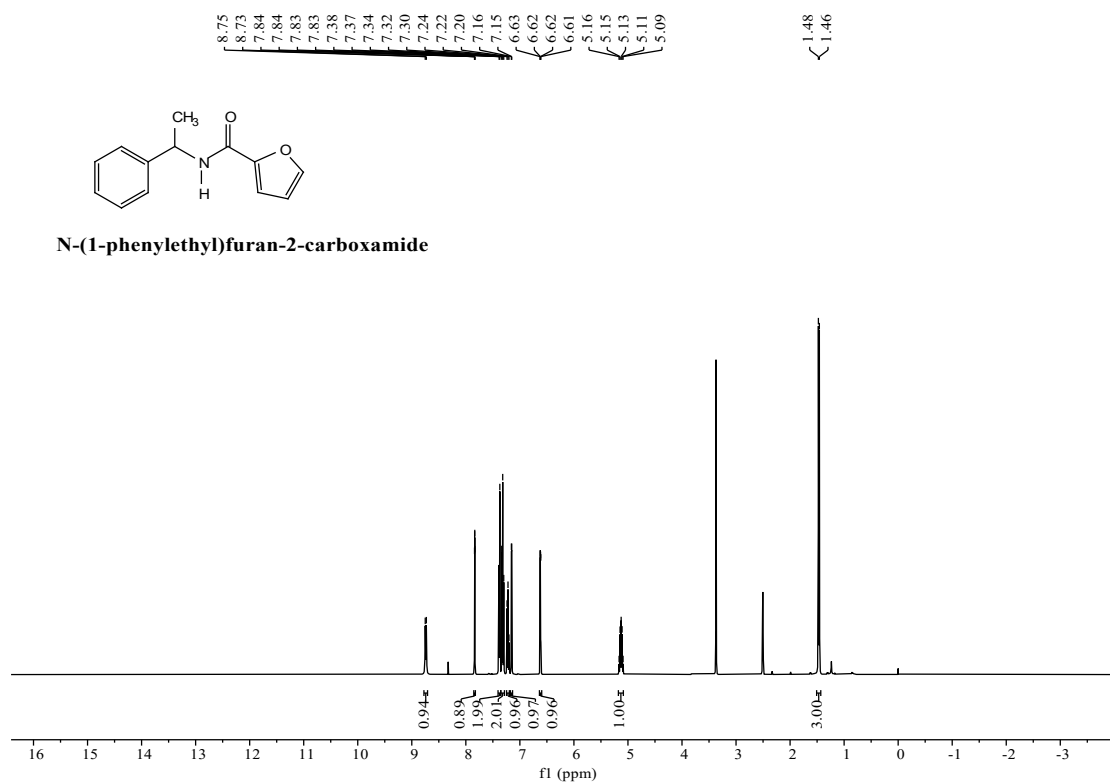


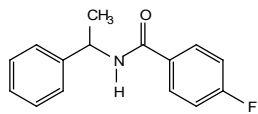


4-chloro-N-(1-phenylethyl)benzamide

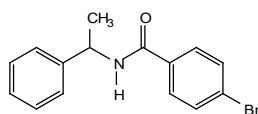
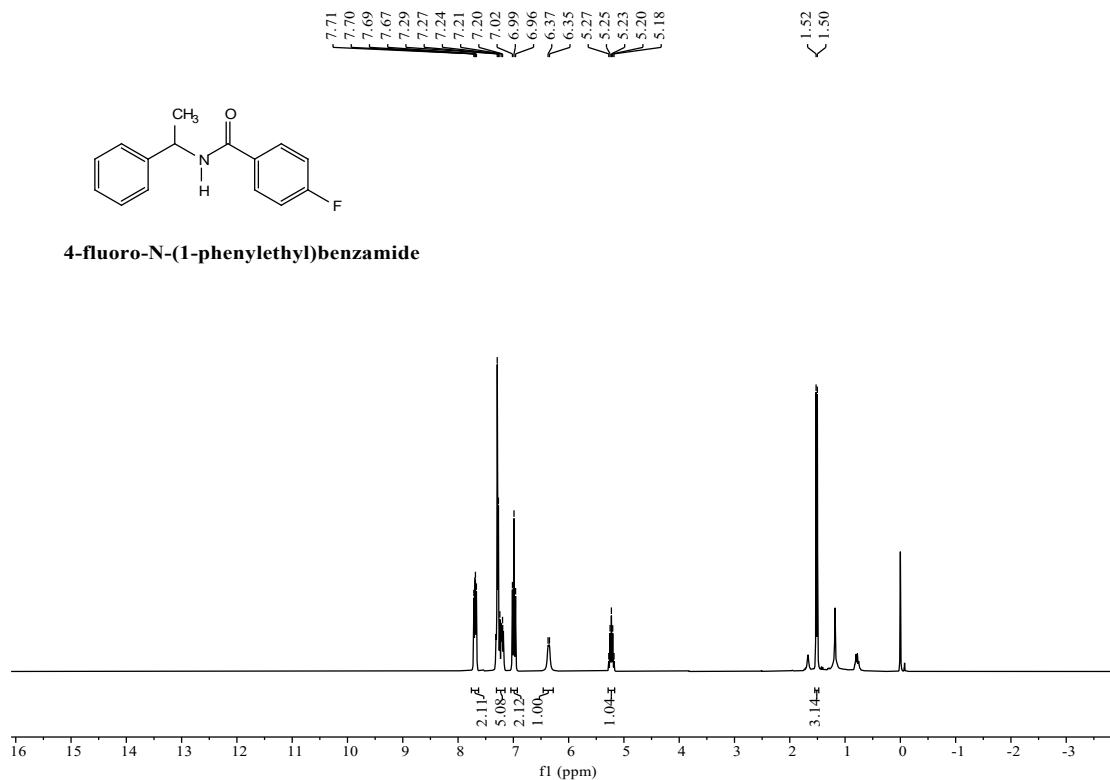


N-(1-phenylethyl)furan-2-carboxamide

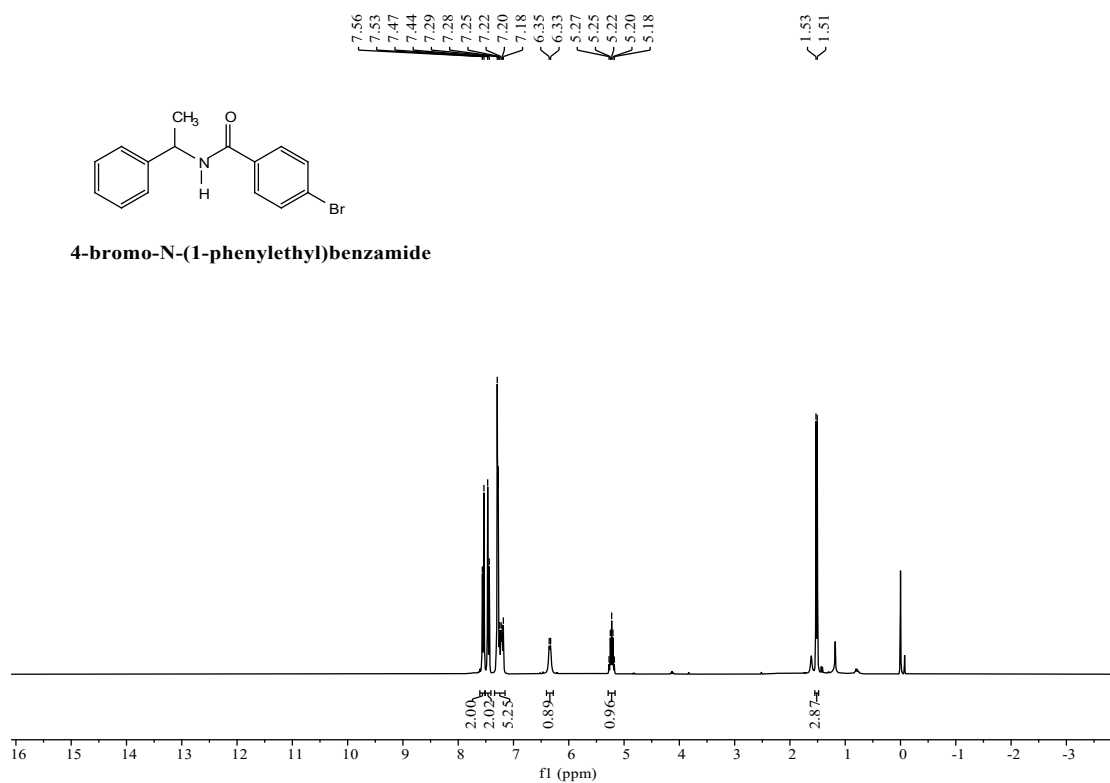


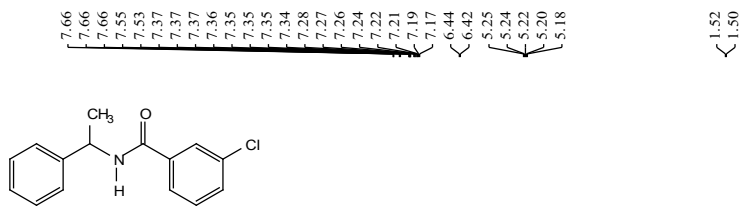


4-fluoro-N-(1-phenylethyl)benzamide

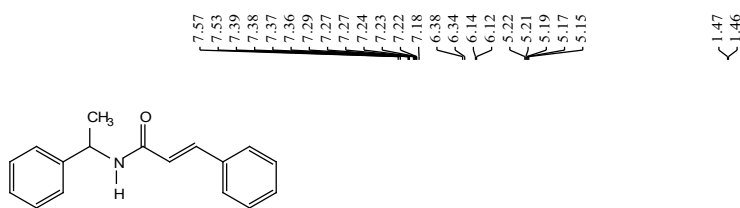
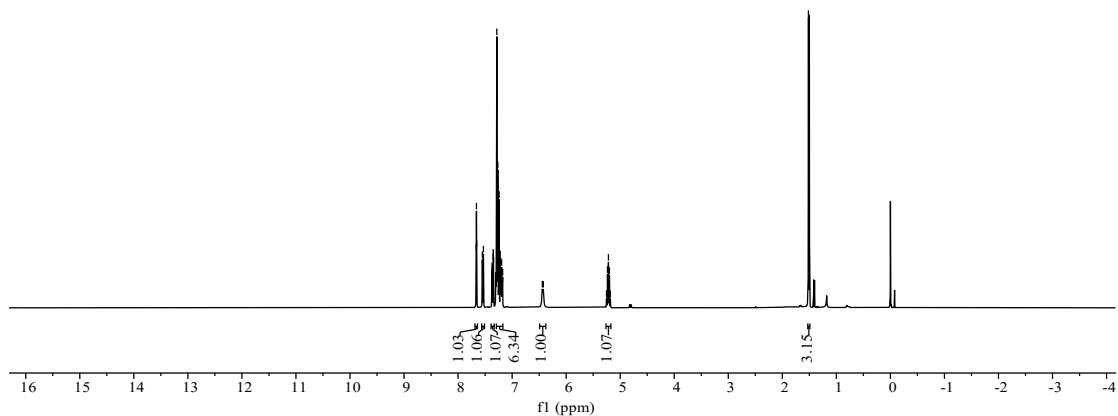


4-bromo-N-(1-phenylethyl)benzamide

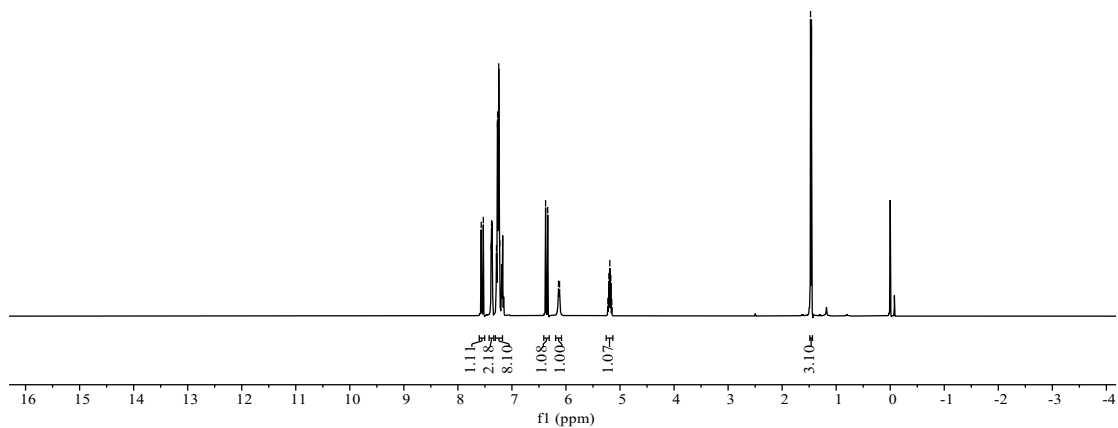


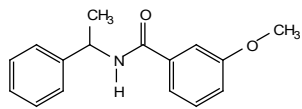


3-chloro-N-(1-phenylethyl)benzamide

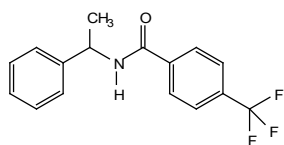
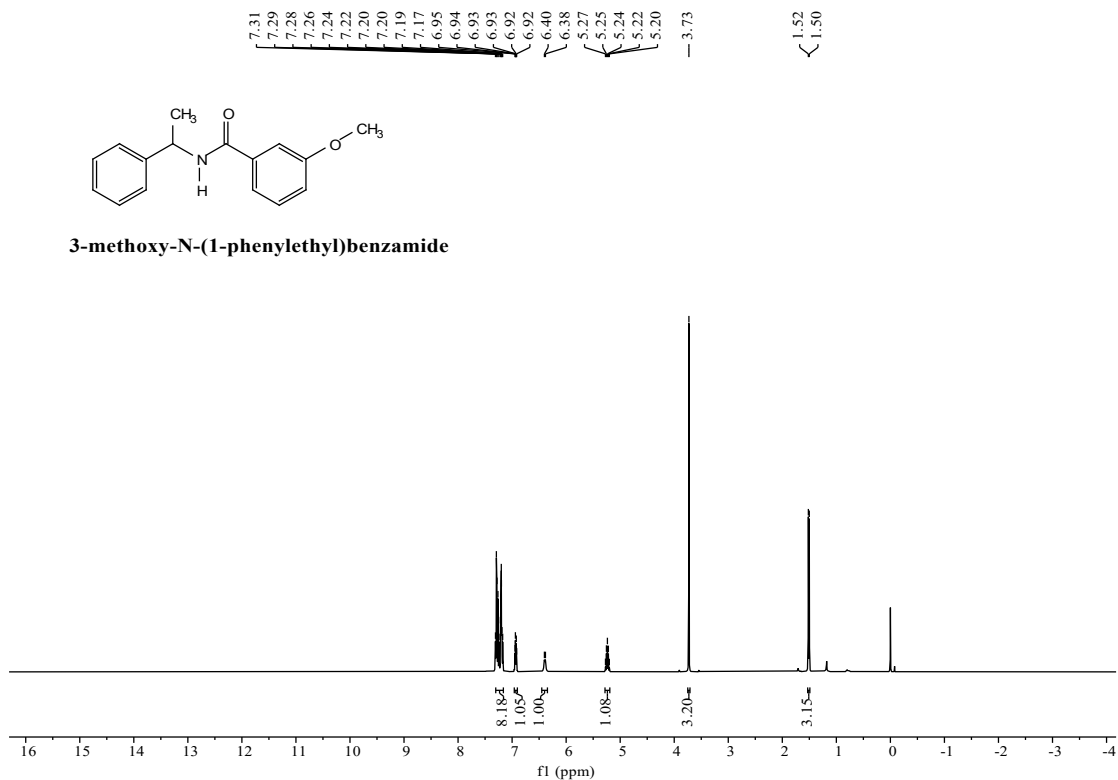


N-(1-phenylethyl)cinnamide

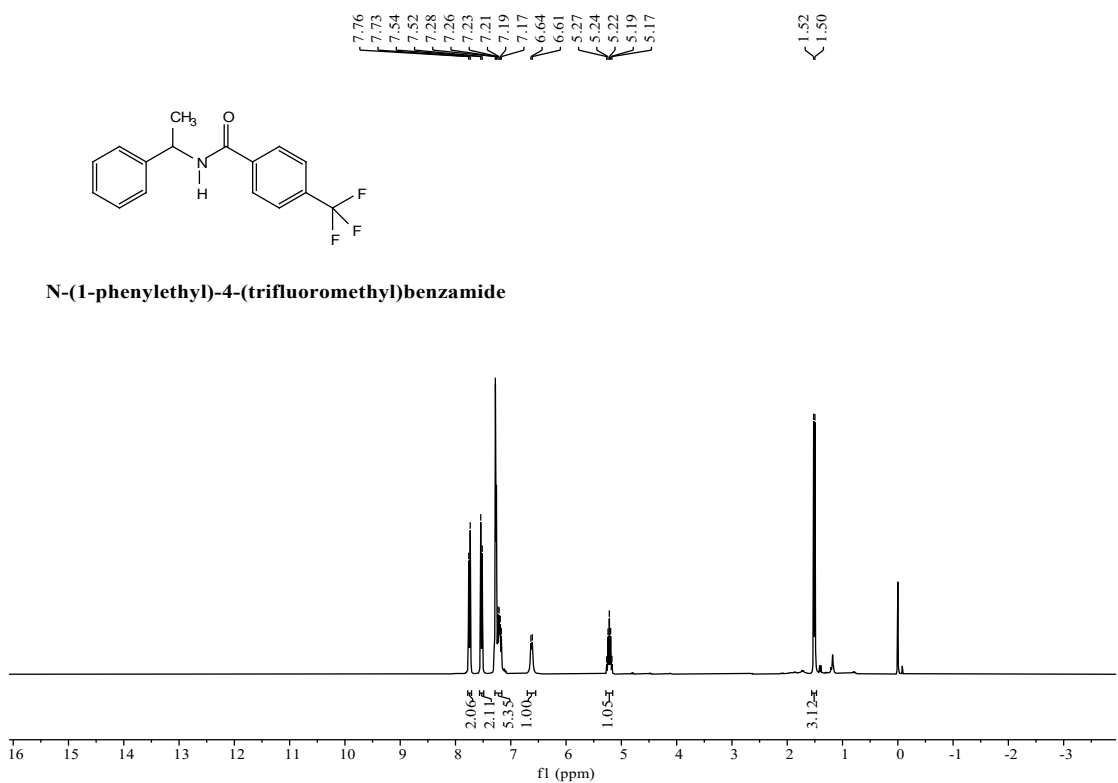


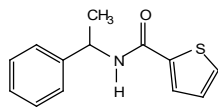


3-methoxy-N-(1-phenylethyl)benzamide

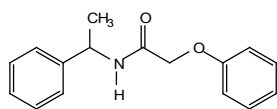
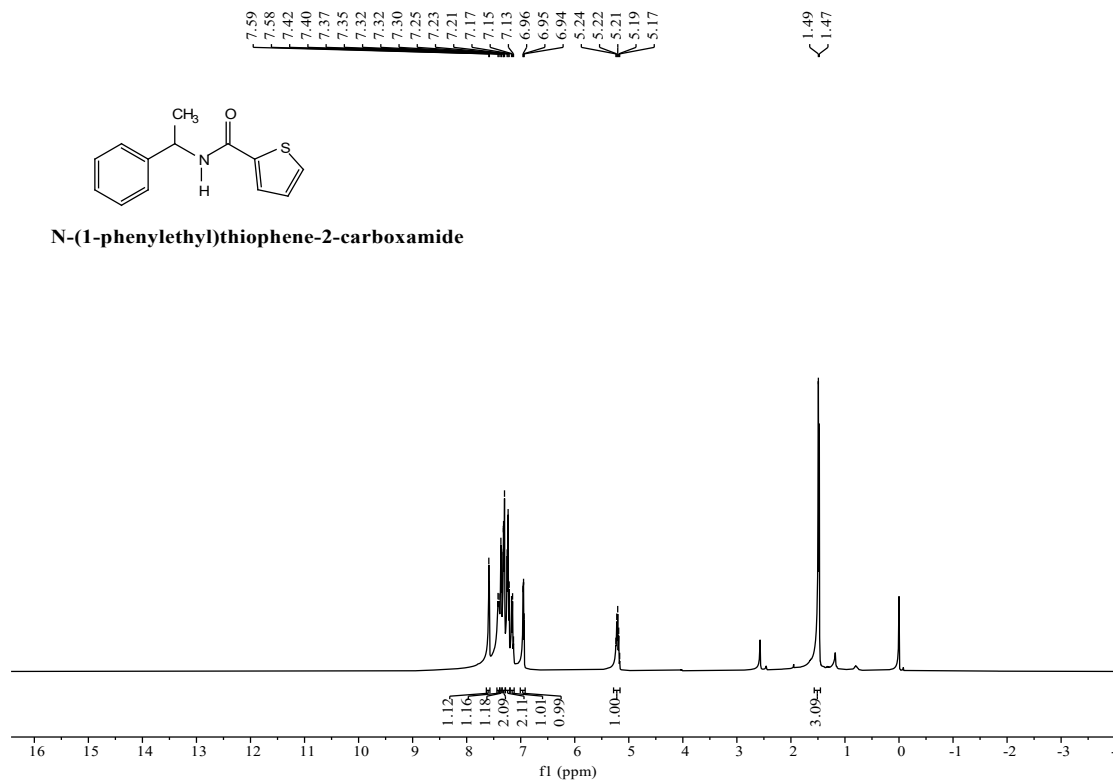


N-(1-phenylethyl)-4-(trifluoromethyl)benzamide

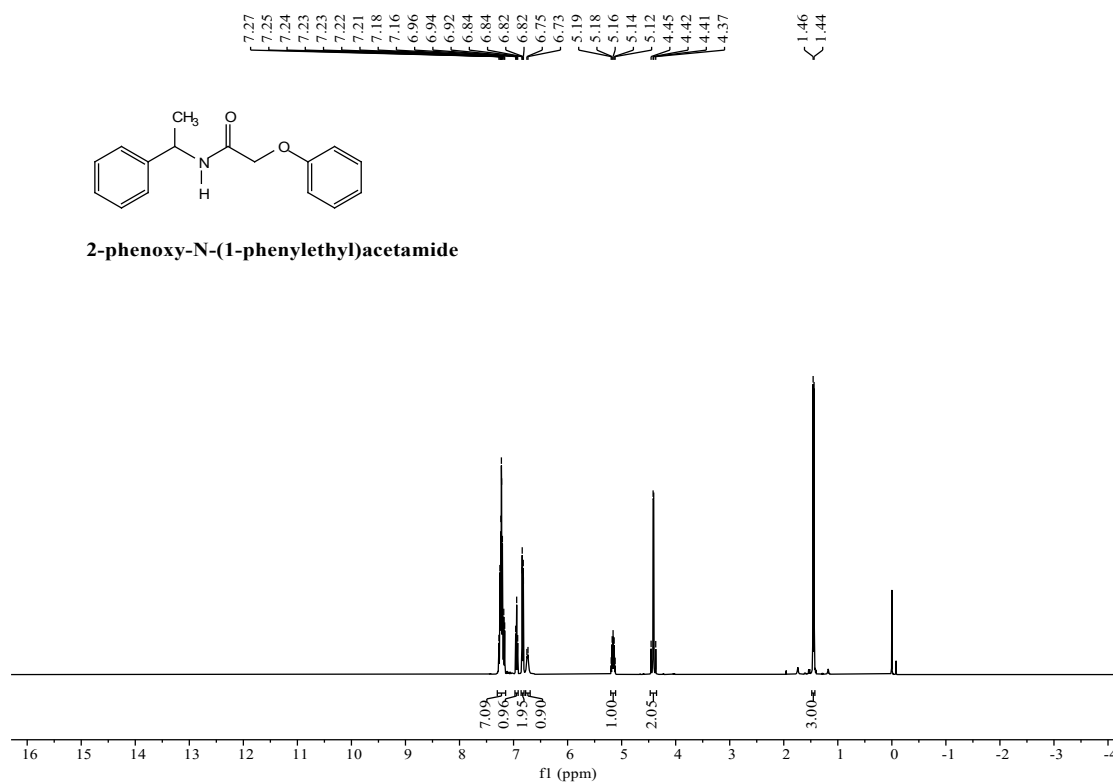


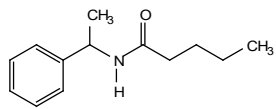


N-(1-phenylethyl)thiophene-2-carboxamide

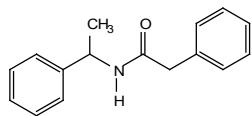
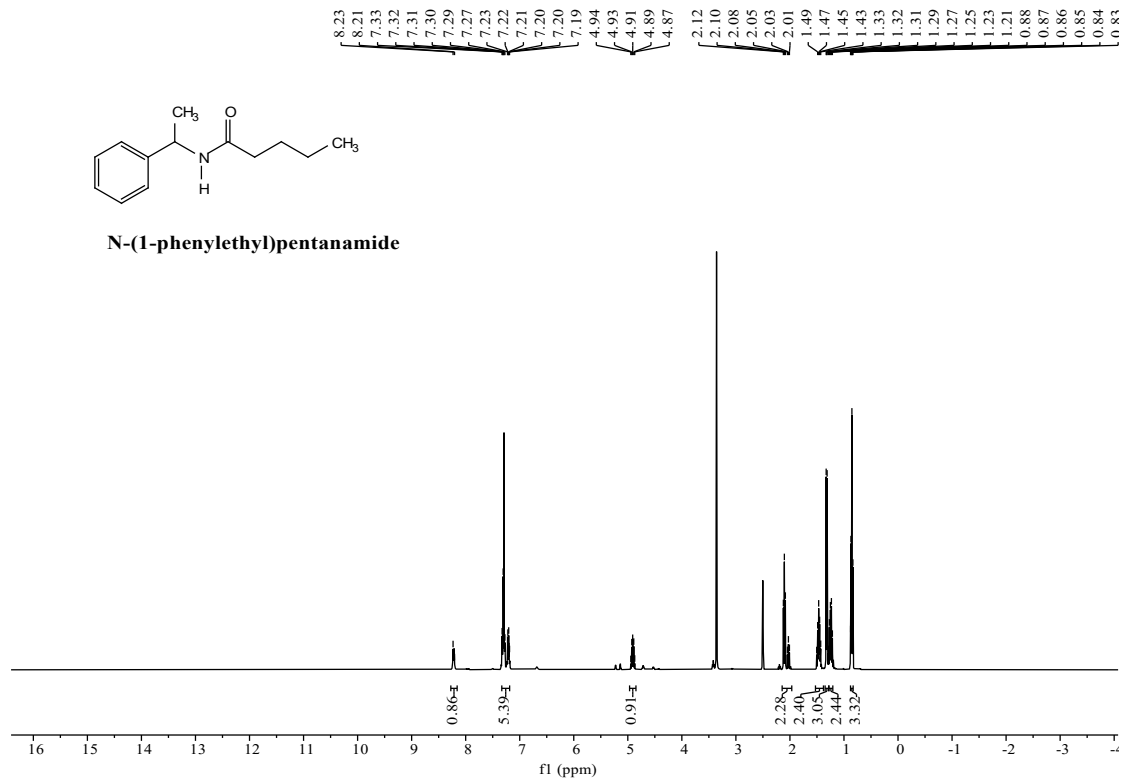


2-phenoxy-N-(1-phenylethyl)acetamide

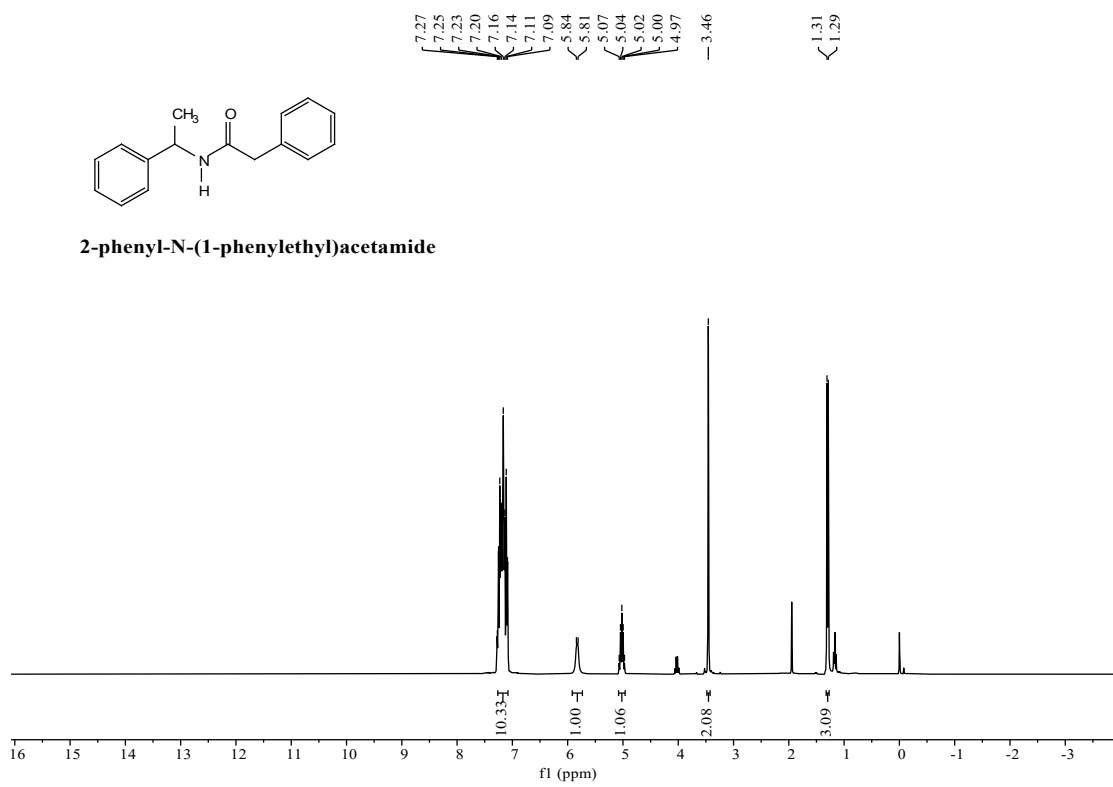


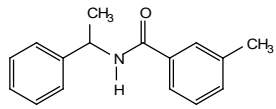


N-(1-phenylethyl)pentanamide

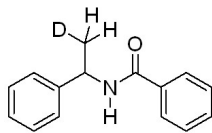
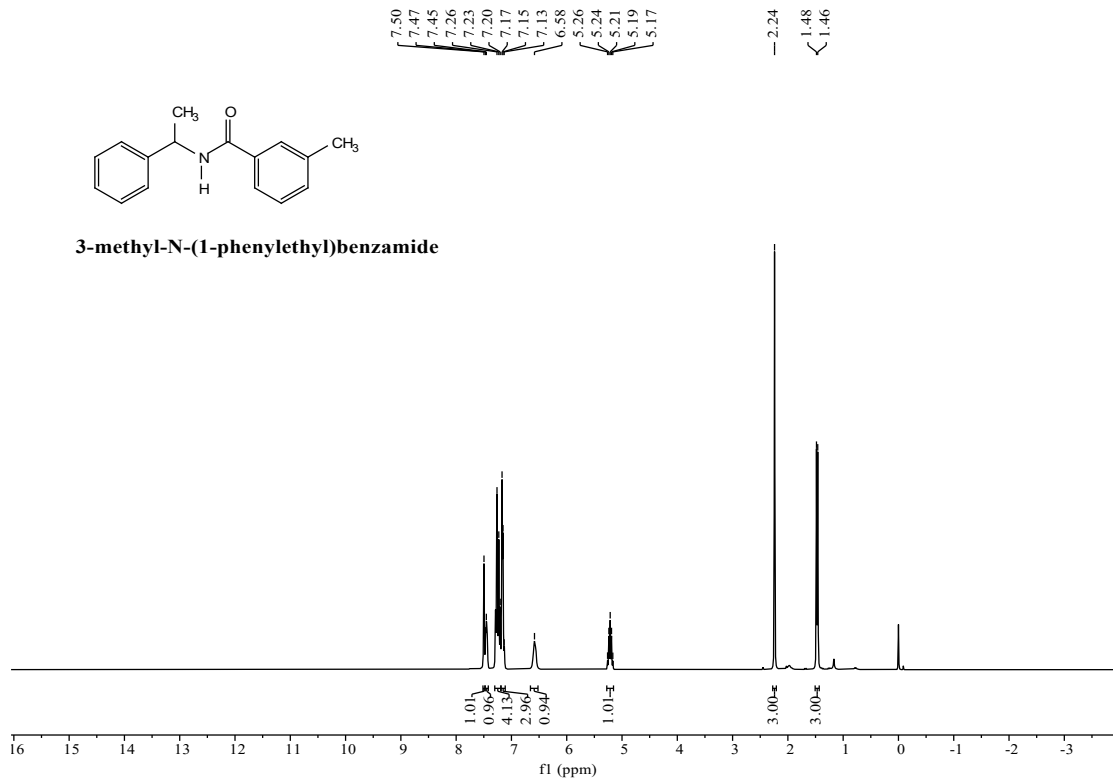


2-phenyl-N-(1-phenylethyl)acetamide

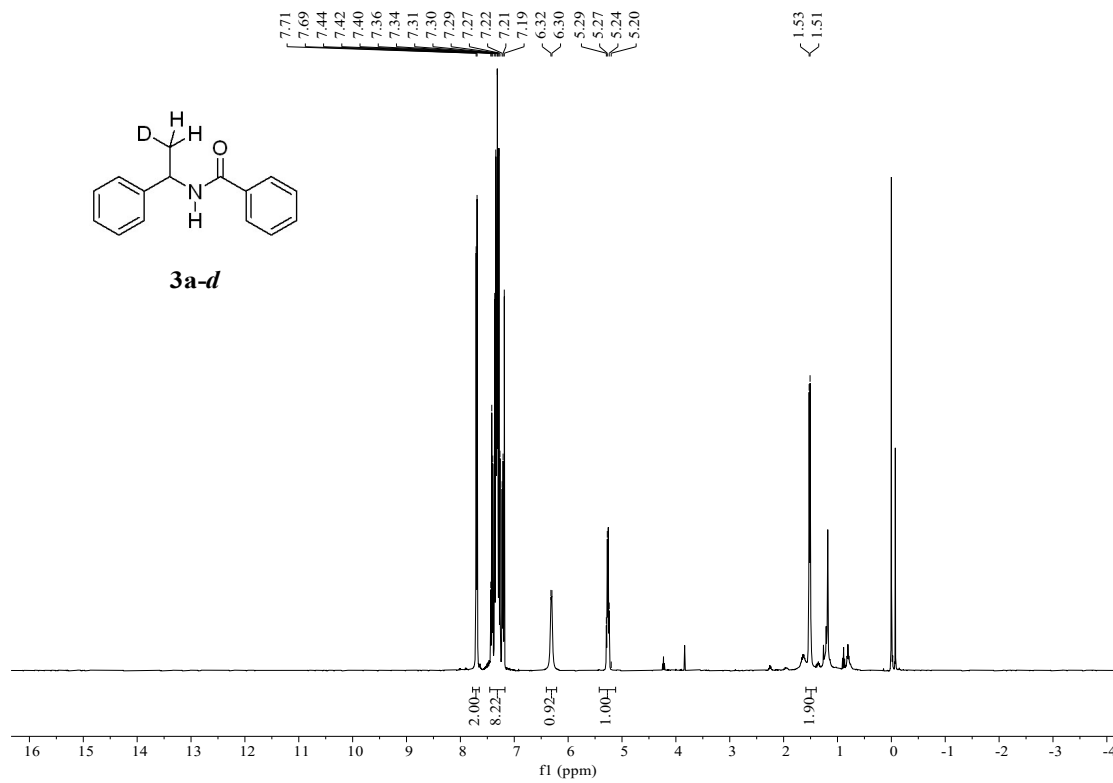


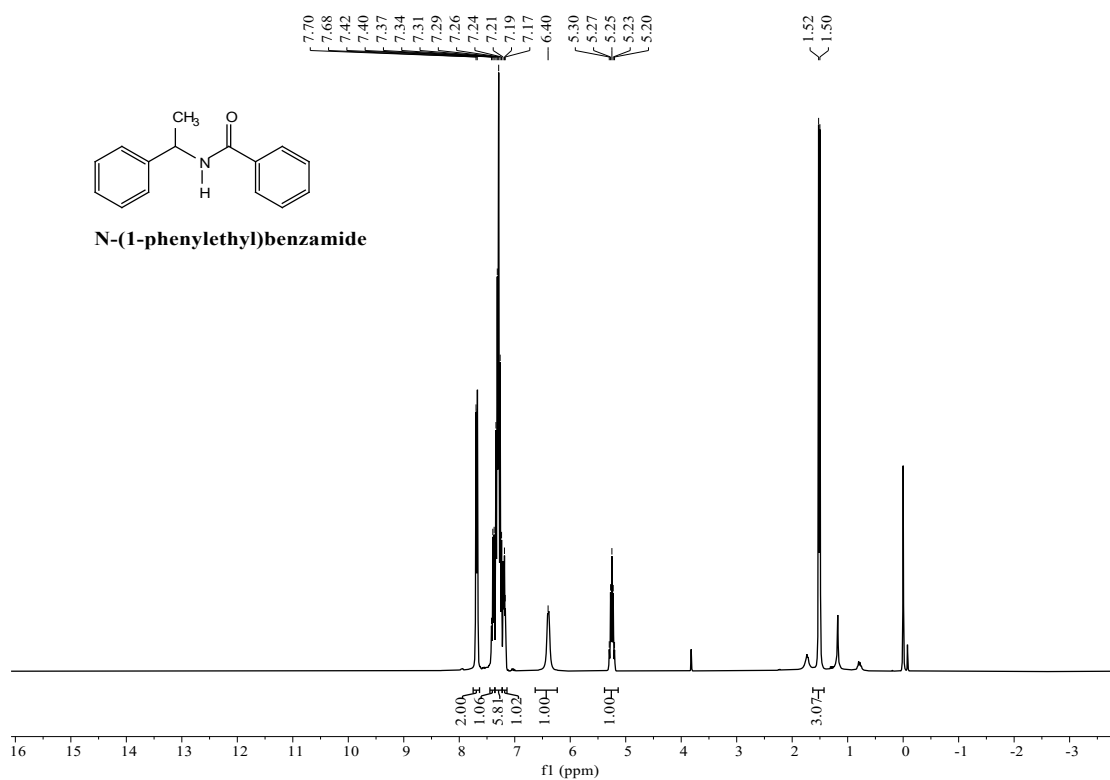
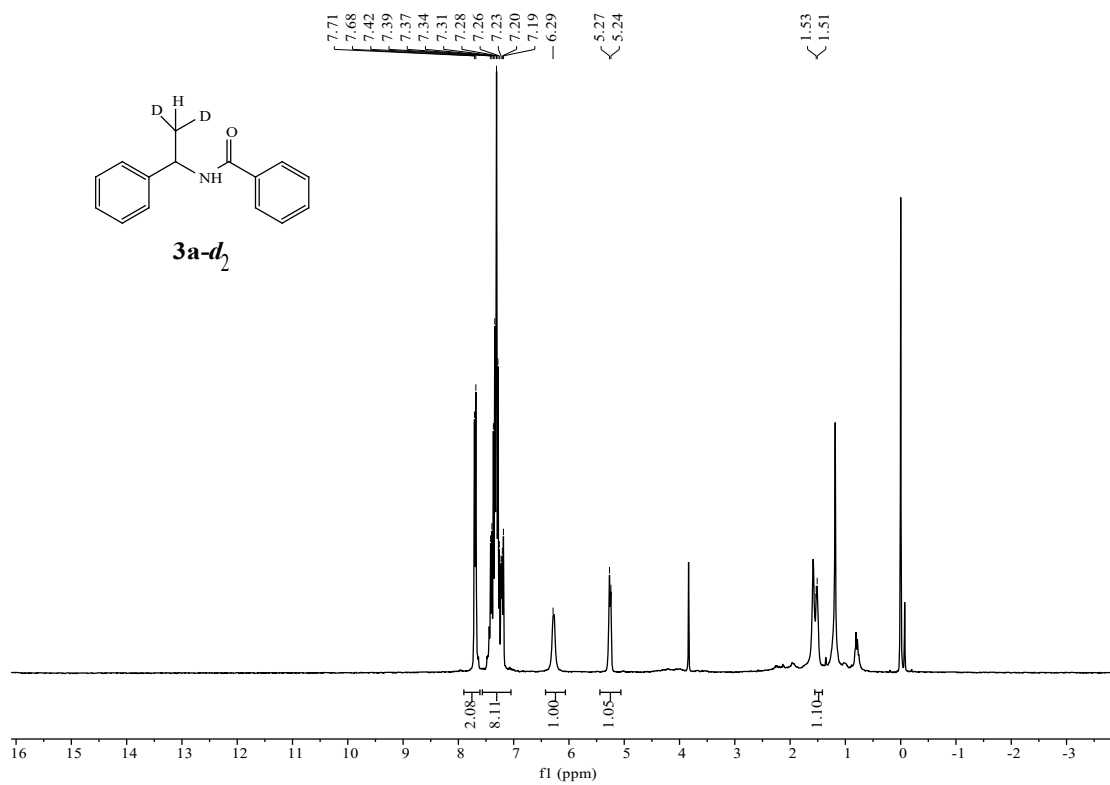


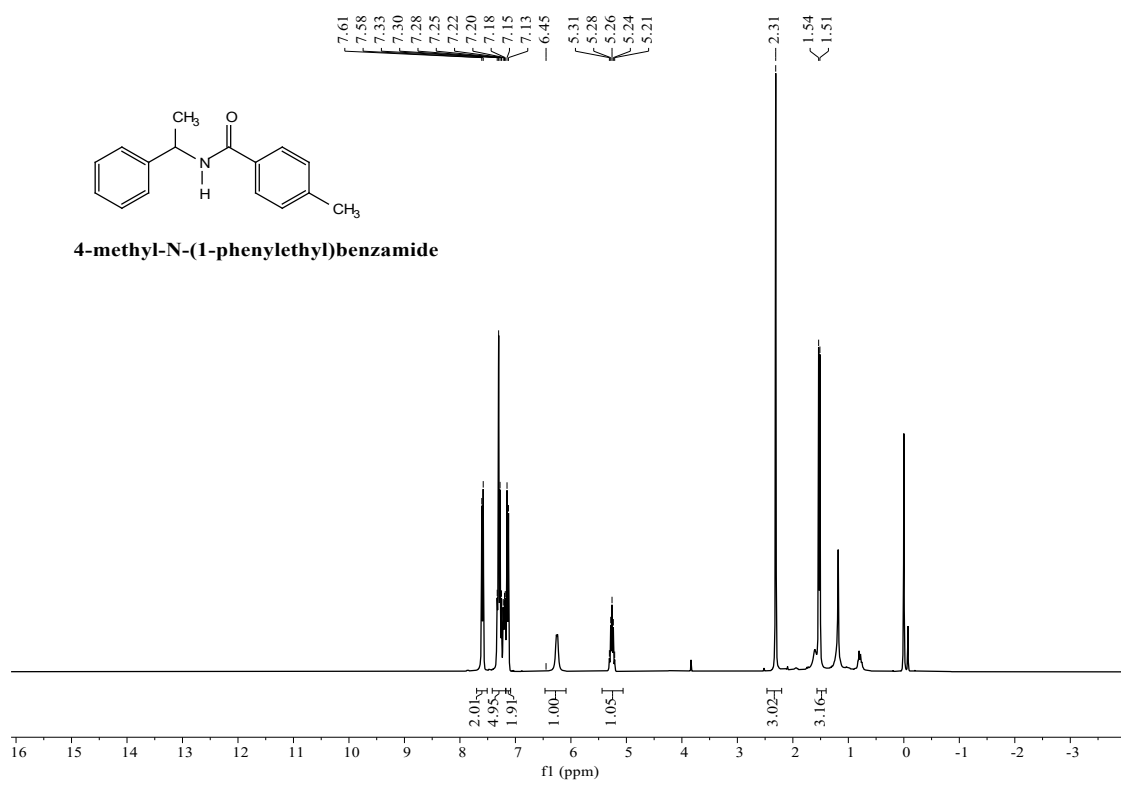
3-methyl-N-(1-phenylethyl)benzamide



3a-d







References

1. P. Jiang, L. Ma, J. Pan, Y. Chun, Q. Xu, J. Dong, *Chinese J. Catal.*, 2009, **30**, 503-508.
2. K. Tang, W. Hou, X. Wang, W. Xu, X. Lu, R. Ma, Y. Fu, W. Zhu, *Micropor. Mesopor. Mat.*, 2021, **328**, 111492-111501.
3. M. Barbero, S. Bazzi, S. Cadamuro, S. Dughera, *Eur. J. Org. Chem.*, 2009, **2009**, 430-436.
4. J. R. Pereira, M. C. Corvo, A. F. Peixoto, A. Aguiar-Ricardo, M. M. B. Marques, *ChemCatChem*, 2023, **15**, e202201318.
5. A. Khalafi-Nezhad, H. O. Foroughi, M. M. Doroodmand, F. Panahi, *J. Mater. Chem.*, 2011, **21**, 12842-12851.
6. S. Yaragorla, G. Singh, P. Lal Saini, M. K. Reddy, *Tetrahedron Lett.*, 2014, **55**, 4657.
7. N. Arıkan Ölmez, B. Osman, *Res. Chem. Intermed.*, 2022, **48**, 4987-5001.
8. B. S. Reddy, N. S. Reddy, C. Madan, J. Yadav, *Tetrahedron Lett.*, 2010, **51**, 4827-4829.